

Probing LLM Hallucination from Within: Perturbation-Driven Approach via Internal Knowledge

Seongmin Lee^{*12}, Hsiang Hsu², Chun-Fu (Richard) Chen², Duen Horng (Polo) Chau¹

¹Georgia Institute of Technology, ²JPMorganChase Global Technology Applied Research
seongmin@gatech.edu, {hsiang.hsu, richard.cf.chen}@jpmchase.com, polo@gatech.edu

Abstract

LLM hallucination, where unfaithful text is generated, presents a critical challenge for LLMs’ practical applications. Current detection methods often resort to external knowledge, LLM fine-tuning, or supervised training with large hallucination-labeled datasets. Moreover, these approaches do not distinguish between different types of hallucinations, which is crucial for enhancing detection performance. To address such limitations, we introduce **hallucination probing**, a new task that classifies LLM-generated text into three categories: *aligned*, *misaligned*, and *fabricated*. Driven by our novel discovery that perturbing key entities in prompts affects LLM’s generation of these three types of text differently, we propose **SHINE**, a novel hallucination probing method that does not require external knowledge, supervised training, or LLM fine-tuning. SHINE is effective in hallucination probing across three modern LLMs, and achieves state-of-the-art performance in hallucination detection, outperforming seven competing methods across four datasets and four LLMs, underscoring the importance of probing for accurate detection.

1 Introduction

Large language models (LLMs) excel at text generation (Wu et al., 2023; Thirunavukarasu et al., 2023) but often produce hallucinations — incorrect or unverifiable content — posing significant risks for practical use (Bohannon, 2023). Detecting such hallucinations is crucial yet challenging due to their plausible appearance (Ji et al., 2023a; Xu et al., 2024b) and diverse types (Zhang et al., 2023c; Ji et al., 2023a). One common detection approach involves comparing outputs with external sources (e.g., Wikipedia) (Lin et al., 2021; Min et al., 2023; Tang et al., 2024), but they fail when such sources are unavailable. Alternative approaches include fine-tuning LLMs to reject ques-

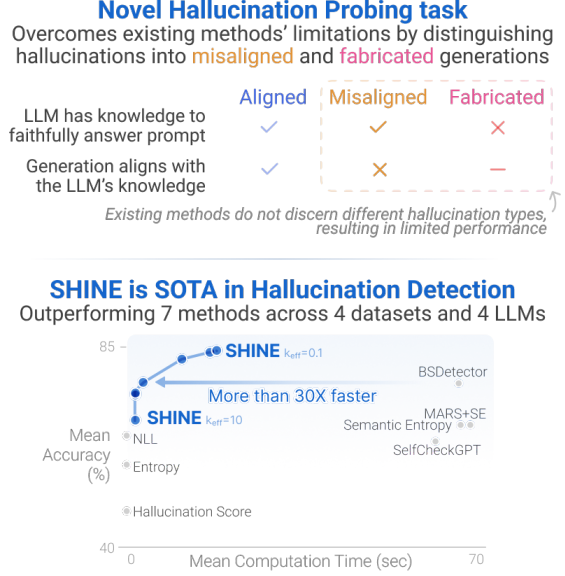


Figure 1: We introduce a novel **hallucination probing** task that distinguishes hallucination into *misaligned* and *fabricated* text. SHINE, our novel hallucination probing method, achieves **best** performance in hallucination detection, outperforming 7 methods across 4 datasets and 4 LLMs (Table 2, 3).

tions likely to produce hallucinations (Zhang et al., 2023a; Xu et al., 2024a; Li et al., 2024) or training classifiers to detect them (Azaria and Mitchell, 2023; Chen et al., 2023; Su et al., 2024), both requiring expensive supervised training on large labeled datasets. To address these limitations, some recent efforts forgo external knowledge or supervised training. These approaches include checking consistency across multiple generations (Manakul et al., 2023), prompting LLMs to assess correctness (Friel and Sanyal, 2023; Zhang et al., 2024b; Chen and Mueller, 2024), or estimating LLM’s uncertainty about its generation (Zhang et al., 2023b; Farquhar et al., 2024; Kossen et al., 2024; Chen et al., 2024; Yadkori et al., 2024a).

However, the methods above have a key limitation: they do not assess whether an LLM possesses sufficient knowledge to generate accurate re-

^{*}Work done during internship at JPMorganChase.

sponses — an essential factor in ensuring accurate detection. Specifically, consistency checks cannot identify hallucinations that the model repeatedly generates (Slobodkin et al., 2023), while prompting approaches may result in random guesses when the LLM lacks knowledge. Moreover, uncertainty-based methods assume all hallucinations stem from uncertainty, neglecting factors such as randomness in token sampling or beam search variability (Stahlberg and Byrne, 2019; Holtzman et al., 2019). These limitations highlight the critical need to assess the LLM’s knowledge and its alignment with generated content. We address this gap with the following key contributions:

- **A novel hallucination probing task** that classifies LLM-generated text into three categories — *aligned* (LLM has sufficient knowledge and responds faithfully), *misaligned* (LLM has knowledge but generates contradictions), and *fabricated* (LLM lacks relevant knowledge). Our categorization refines hallucination types beyond existing work (Huang et al., 2023a; Zhang et al., 2023c) (§3), significantly boosting detection performance (Fig. 1).
- **Entity Perturbation Impact discovery**, our key finding revealing that perturbing key entities in prompts affects LLM outputs differently depending on the type of hallucination present (§3). While prior studies have identified that hallucinations arise from errors while retrieving knowledge about the key entities (Ferrando et al., 2024), they did not leverage this for hallucination detection. We systematically perturb key entities to assess their impact on generated tokens, demonstrating how these perturbations can determine whether the generated tokens stem from the LLM’s knowledge and align with it. This provides the foundation for distinguishing between aligned, misaligned, and fabricated responses for hallucination probing.
- **SHINE, a novel hallucination probing method** leveraging our *Entity Perturbation Impact* discovery to predict whether an LLM possesses sufficient knowledge to generate a faithful response and whether the response aligns with the knowledge (§4, Fig. 3). SHINE operates without external knowledge, supervised training, or LLM fine-tuning. SHINE stands for **S**ystematic **H**allucination **I**nspection with **N**oisy **E**ntity.
- **Extensive experiments demonstrating the superiority of our method** on four mod-

ern LLMs (LLaMA2-13B-Chat, LLaMA3-8B-Instruct, Mistral-7B-Instruct, Qwen2.5-7B-Instruct) across four datasets for diverse text generation tasks. Our method effectively classifies aligned, misaligned, and fabricated text (§5.1) and outperforms all existing algorithms on hallucination detection (§5.2), underscoring the importance of hallucination probing.

2 Related Work

Hallucination Probing. Previous studies have examined hallucination causes by inspecting training data, algorithms, and inference process (Sec 3 of (Huang et al., 2023a)). Key issues during inference include contradictions with the LLM’s knowledge — arising from its tendency to prioritize user preferences over accuracy, randomness in generation, and dependency on earlier tokens — and overconfident fabrication despite lacking knowledge (Sec 4 of (Zhang et al., 2023c)). Based on this, we categorize hallucinations into two classes: (1) misaligned, where the LLM has sufficient knowledge but produces contradictions, and (2) fabricated, caused by the LLM’s lack of knowledge. Our work does not aim to attribute hallucination causes to model components (Chen et al., 2025).

Hallucination Detection. Some approaches verify LLM-generated text using external sources or human evaluation, which can be unavailable or costly (Lin et al., 2021; Min et al., 2023; Tang et al., 2024). As an alternative, researchers trained classifiers to detect hallucinations (Chen et al., 2023; Azaria and Mitchell, 2023; Su et al., 2024) or fine-tuned LLMs to avoid potentially hallucinated responses (Zhang et al., 2023a; Xu et al., 2024a; Li et al., 2024), but these require training on large labeled datasets. Prompting (Friel and Sanyal, 2023; Li et al., 2023; Zhang et al., 2024b) or consistency checks (Manakul et al., 2023; Yadkori et al., 2024a,b; Chen et al., 2024) may fail against confident fabrications (Bengio et al., 2015; Iqbal and Qureshi, 2022; Zhang et al., 2023b; Kamath et al., 2024). Uncertainty estimation methods (Huang et al., 2023b; Quevedo et al., 2024; Zhang et al., 2023b; Farquhar et al., 2024; Hou et al., 2024; Bakman et al., 2024; Yaldiz et al., 2024; Liu et al., 2025) often overlook hallucinations from randomness or token dependencies (Stahlberg and Byrne, 2019; Holtzman et al., 2019; Zhang et al., 2024a). We propose a new direction to more accurately identify hallucinations without any external knowledge, training, or impractical assumptions.

3 Discovery: Entity Perturbation Impact for Hallucination Probing

Inspired by prior work that explores GPT-2’s knowledge by perturbing entities in templated prompts (Meng et al., 2022), we ask: *Is LLM-hallucinated text, ungrounded in model knowledge, as sensitive to perturbations as aligned text?* This drives our novel Entity Perturbation Impact discovery, forming the basis of SHINE, our hallucination probing method (§4). To explore this, we extend the analysis to modern LLMs, specifically, LLaMA2-13B-Chat-GPTQ (Touvron et al., 2023) (henceforth, LLaMA2), and more flexible prompts that ask factual questions about specific entities, which have been the primary focus of recent research (Martino et al., 2023; Sun et al., 2023; Ferrando et al., 2024; Huang et al., 2024). We use the NEC benchmark (Liu et al., 2024a), which includes prompts about real and fictional entities across six topics; real-entity prompts yield aligned or misaligned responses, whereas fictional ones generate fabricated responses (details in §A.1).

Below, we outline an LLM’s inference process, then introduce our perturbation and evaluation method, which leads to our key discovery that perturbing key entities affects LLM’s generation of aligned, misaligned, and fabricated responses differently, and ultimately gives rise to SHINE (§4).

LLM inference without perturbation. For a prompt P and text G , a tokenizer with a token set \mathcal{T} splits P into M tokens $t_{1:M} = [t_1, \dots, t_M]$ and G into N tokens $t_{M+1:M+N} = [t_{M+1}, \dots, t_{M+N}]$, where $t_i \in \mathcal{T}$. Each token t_i is mapped to a d -dimensional embedding vector $\mathbf{e}_i \in \mathbb{R}^d$ by a token embedding map. An LLM f takes the embedding vector sequence $\mathbf{e}_{1:M+N} = [\mathbf{e}_1, \dots, \mathbf{e}_{M+N}]$ as an input and computes the probability of each token appearing after each token position i ; i.e., $f(\mathbf{e}_{1:M+N}) = \mathbf{P}_{1:M+N} \in \mathbb{R}^{(M+N) \times |\mathcal{T}|}$, where $\mathbf{P}_i \in \mathbb{R}^{|\mathcal{T}|}$ and $\mathbf{P}_i(t)$ is the probability of the token t to be generated at the position $i + 1$. We summarize these notations in App. H.

Entity Perturbation. For each prompt P , we manually identify the key entity S , tokenized as $t_{1:K}^S$. We locate all token positions I_S where S appears in P and the LLM’s response G , i.e., $I_S = \{i | t_{i:i+K-1} = S\}$. To perturb the embeddings of S , we add Gaussian noise $\epsilon \sim \mathcal{N}(0, (3\sigma_0)^2) \in \mathbb{R}^{K \times d}$ to all occurrences of S , where σ_0 is the standard deviation of token embeddings in the NEC dataset (Meng et al., 2022); i.e., $\hat{\mathbf{e}}_{i:i+K-1} =$

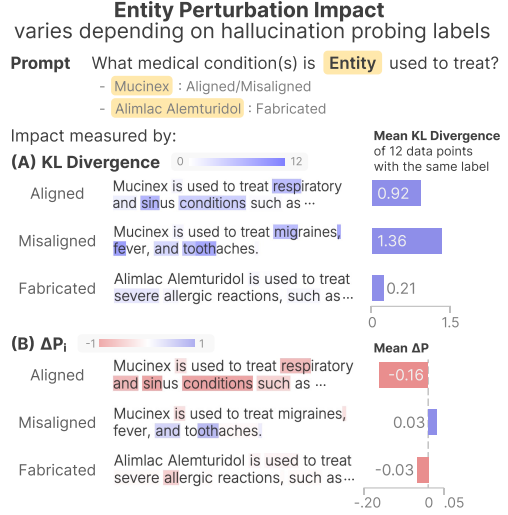


Figure 2: Entity Perturbation Impact, measured by KL divergence and ΔP_i , varies across aligned, misaligned, and fabricated text. **(A)** Tokens in aligned and misaligned text, strongly linked to the LLM’s knowledge of the entity, have high KL divergence, while most tokens in fabricated text have near-zero values, indicating weak association with the LLM’s knowledge. The mean KL divergence of fabricated text is significantly lower than aligned and misaligned text. **(B)** While tokens in aligned and fabricated text generally show negative or near-zero ΔP_i , misaligned text has tokens with positive ΔP_i , particularly those in the contradictory phrase, leading the mean ΔP of misaligned text to surpass that of aligned and fabricated text.

$\mathbf{e}_{i:i+K-1} + \epsilon$ for $i \in I_S$, while leaving other token embeddings unchanged. Then, we input $\hat{\mathbf{e}}_{1:M+N}$ to the LLM f , obtaining a perturbed probability distribution $\hat{\mathbf{P}}_{1:M+N} = f(\hat{\mathbf{e}}_{1:M+N}) \in \mathbb{R}^{(M+N) \times |\mathcal{T}|}$. For each token position i in G , we evaluate the Entity Perturbation Impact using: (1) Kullback-Leibler (KL) divergence between \mathbf{P}_i and $\hat{\mathbf{P}}_i$ (i.e., $KL(\mathbf{P}_i \parallel \hat{\mathbf{P}}_i)$) to capture global effects across the entire vocabulary and (2) change in the generation probability of token t_i (i.e., $\Delta P_i = \hat{\mathbf{P}}_i(t_i) - \mathbf{P}_i(t_i)$), focusing on generated tokens. To mitigate the impact of random Gaussian noise, we repeat this process 10 times with different random seeds.

Our approach differs from methods that detect hallucinations via inconsistencies across generations. While their inconsistencies mean that there is a token position i with multiple inconsistent token t s with high generation probability $\mathbf{P}_i(t)$, we measure the distance between original and perturbed distributions \mathbf{P}_i and $\hat{\mathbf{P}}_i$.

Experiments. From the NEC dataset, we randomly sample two prompts for each topic for both existent and non-existent entities, yielding 12 aligned, 12 misaligned, and 12 fabricated data points. This

analysis focuses on a small subset, as it requires manual identification of key entities; results for full dataset using our automated approach are in §5. We also evaluate each text G 's Entity Perturbation Impact by taking mean across all tokens in G except those of the perturbed entity, and refer to the results as the KL divergence and ΔP .

Fig. 2 demonstrates the Entity Perturbation Impact of aligned, misaligned, and fabricated text (additional results in App. F). Fabricated text shows a much lower mean KL divergence (0.21) than aligned (0.92) and misaligned (1.36) text (Fig. 2A). For example, in the aligned response to the prompt “What medical condition(s) is Mucinex used to treat?”, tokens for *respiratory* and *sinus*, which are relevant to *Mucinex*, have high KL divergence, whereas fabricated text’s tokens exhibit near-zero KL divergence, indicating their weak association with the LLM’s knowledge. Moreover, misaligned text contains tokens with positive ΔP_i , with a mean ΔP of 0.03 — higher than aligned (-0.16) and fabricated (-0.03) text, where most tokens have negative or near-zero ΔP_i (Fig. 2B). In the misaligned text about *Mucinex*, tokens in the misaligned phrase *fever, and toothaches* show positive ΔP_i , suggesting $\Delta P_i > 0$ as a misalignment indicator.

Key Takeaways. Low Entity Perturbation Impact measured by KL divergence strongly indicates fabricated text, as its tokens are weakly tied to key entities. In contrast, a rise in generation probability after perturbation ($\Delta P > 0$) signals misalignment. This is because aligned tokens are grounded in model knowledge of the key entities, so perturbation lowers their probability ($\Delta P < 0$), while tokens in fabricated text remains unaffected ($\Delta P \approx 0$). In §4, we introduce SHINE, a hallucination probing method that leverages Entity Perturbation Impact to distinguish between aligned, misaligned, and fabricated text.

4 SHINE: Hallucination Probing Method

Leveraging our Entity Perturbation Impact discovery (§3), we develop a two-stage workflow for hallucination probing, consisting of *Model Knowledge Test* and *Alignment Test* (Fig. 3). The Model Knowledge Test first assesses whether the LLM has enough knowledge to generate faithful response for the prompt and distinguishes fabricated text from other two types (§4.1). Then, the Alignment Test examines whether the generated text aligns with the LLM’s knowledge, classifying it as either aligned or misaligned (§4.2).

4.1 Model Knowledge Test

Model Knowledge Test builds on our discovery that fabricated text exhibits much lower Entity Perturbation Impact (KL divergence) than aligned or misaligned text. To systematically identify key entities, we detect all entities in a prompt and perturb them with varying strength, determined by attention they receive. The Model Knowledge Test involves four steps: identifying entity, determining perturbation strength, perturbing entity embeddings, and measuring perturbation impact.

Step 1. Entity Identification. Using the named entity and noun chunk extraction of SpaCy (Honnibal and Montani, 2017), Model Knowledge Test extracts entities S_1, \dots, S_L in P (details in App. G).

Step 2. Perturbation Strength Computation. To prioritize influential entities, we apply stronger perturbations to entities with higher attention. To calculate the attention $att_l \in \mathbb{R}^+$ of each entity S_l (Tu et al., 2021), we concatenate tokens in P and G into $t_{1:M+N}$, feed the token sequence into the LLM, and sum the attention values received by the tokens of S_l while generating $t_{M+1:M+N}$. We then scale att_l into $a_l \in [0, 1]$:

$$a_l = \frac{\exp(k_{att} \cdot att_l)}{\exp(k_{att} \cdot \max(att_1, \dots, att_L))}, \quad (1)$$

where $k_{att} \geq 0$ controls the impact of attention values; $k_{att} = 0$ weighs all entities equally, while larger values emphasize highly attended entities.

Since LLMs tend to fabricate for entities with low frequency in the training data (Mallen et al., 2023; Kandpal et al., 2023; Min et al., 2023; Ji et al., 2023b), we further adjust perturbation strength using the generation likelihood of each entity S_l , which serves as a good proxy for frequency (Hartmann et al., 2023). Specifically, we use the negative log-likelihood, scaled by token position to consider later tokens’ importance. For an entity S_l , tokenized as $t_{1:K_l}^{S_l}$, the perturbation strength $w_l \in \mathbb{R}^+$ is calculated as

$$w_l = a_l \cdot \left(1 - \frac{1}{K_l} \sum_{k=1}^{K_l} \sqrt{k-1} \log Pr(t_k^{S_l} | t_{1:k-1}^{S_l}) \right)^{-1}. \quad (2)$$

Step 3. Entity Perturbation. We perturb L entities by adding noise to their token embeddings. For entity $S_l = t_{1:K_l}^{S_l}$, we identify all token positions I_{S_l} where it appears in (P, G) : $I_{S_l} = \{i | t_{i:i+K_l-1} = S_l\}$. We add Gaussian noise $\epsilon_l^{MKT} \sim \mathcal{N}(0, (\sigma_l^{MKT})^2) \in \mathbb{R}^{K_l \times d}$ to all $i \in I_{S_l}$, i.e., $\mathbf{e}_{i:i+K_l-1}^{MKT} = \mathbf{e}_{i:i+K_l-1} + \epsilon_l^{MKT}$, while leaving other tokens unchanged; the standard deviation

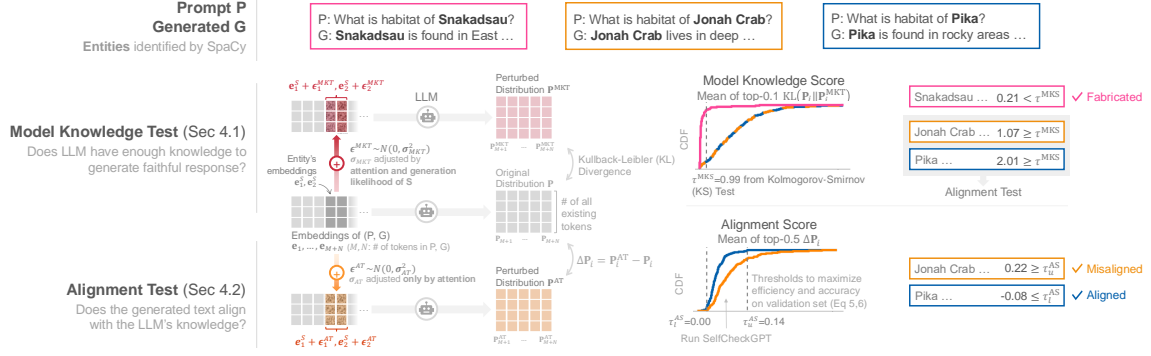


Figure 3: SHINE classifies LLM-generated text into aligned, misaligned, and fabricated through two steps: Model Knowledge Test (§4.1) and Alignment Test (§4.2). The Model Knowledge Test identifies whether the LLM has sufficient knowledge to generate a faithful response by perturbing entities in the prompt and evaluating the impact; fabricated text is differentiated at this stage. For the data that the LLM has enough knowledge, we conduct the Alignment Test to examine whether the text aligns with the LLM’s knowledge.

$\sigma_l^{MKT} = w_l \cdot \sigma$, where σ is a hyperparameter (details in §5). We input the perturbed embeddings $\mathbf{e}_{1:M+N}^{MKT}$ to the LLM to compute the perturbed probability distribution $\mathbf{P}^{MKT} = f(\mathbf{e}_{1:M+N}^{MKT}) \in \mathbb{R}^{(M+N) \times |\mathcal{T}|}$.

Step 4. Model Knowledge Score Evaluation. We compute KL divergence between \mathbf{P} and \mathbf{P}^{MKT} at each token position i in the generated text G and refer to it as Model Knowledge Score at the position i , which is denoted as $MKS_i = KL(\mathbf{P}_i \| \mathbf{P}_i^{MKT})$. As the dependency on the previous tokens can reduce the KL divergence values of some tokens (details in App. F), we evaluate MKS , the Model Knowledge Score of G , by taking the mean of top- p^{MKS} values of MKS_i for $i = M+1, \dots, M+N$ ($0 < p^{MKS} \leq 1$):

$$MKS = \frac{1}{[p^{MKS} \cdot N]} \sum_{i=1}^{[p^{MKS} \cdot N]} MKS_i^{sort}, \quad (3)$$

where $MKS_1^{sort} \geq \dots \geq MKS_N^{sort}$ is a sorted permutation of $MKS_{M+1}, \dots, MKS_{M+N}$. We repeat this 10 times with different random seeds. If the Model Knowledge Score is lower than a threshold, we classify the text as fabricated; otherwise, we proceed to the Alignment Test (§4.2). We determine the threshold τ^{MKS} using the Kolmogorov-Smirnov (KS) test (Massey Jr, 1951) on the validation set: $\tau^{MKS} = \arg \max_{\tau \in [0, \infty)} (\mathbf{F}_f^{MKS}(\tau) - \mathbf{F}_{a,m}^{MKS}(\tau))$, where \mathbf{F}_f^{MKS} is the cumulative probability of fabricated data’s Model Knowledge Score and $\mathbf{F}_{a,m}^{MKS}$ is that of aligned or misaligned data.

4.2 Alignment Test

After ensuring the LLM has enough knowledge about (P, G) via Model Knowledge Test, we check

if the text G aligns with that knowledge. Specifically, we add noise $\epsilon_l^{AT} \sim \mathcal{N}(0, (\sigma_l^{AT})^2)$ to the embeddings of each entity S_l to compute the perturbed embeddings $\mathbf{e}_{1:M+N}^{AT}$; since Model Knowledge Test has already verified that the model is knowledgeable about S_l , we do not use the likelihood but adjust σ_l^{AT} only with a_l as $\sigma_l^{AT} = a_l \cdot \sigma$, where σ is the same hyperparameter used in Model Knowledge Test. We then compute the perturbed probability distribution $\mathbf{P}^{AT} = f(\mathbf{e}_{1:M+N}^{AT}) \in \mathbb{R}^{(M+N) \times |\mathcal{T}|}$ and $\Delta P_i = \mathbf{P}_i^{AT}(t_i) - \mathbf{P}_i(t_i)$ for $i = M+1, \dots, M+N$.

Since some tokens in the misaligned text can still be aligned with model knowledge, while all tokens in the aligned text should be aligned, we evaluate Alignment Score (AS) by taking the mean of top- p^{AS} ΔP_i values ($0 < p^{AS} \leq 1$):

$$AS = \frac{1}{[p^{AS} \cdot N]} \sum_{i=1}^{[p^{AS} \cdot N]} \Delta P_i^{sort}, \quad (4)$$

where $\Delta P_1^{sort} \geq \dots \geq \Delta P_N^{sort}$ is a permutation of $\Delta P_{M+1}, \dots, \Delta P_{M+N}$ sorted in descending order.

While large negative and large positive AS values indicate alignment and misalignment, respectively, $AS \approx 0$ can imply either. To handle near-zero AS , we use SelfCheckGPT (Manakul et al., 2023), which takes some computational cost but effectively differentiates text about which a model has enough knowledge. We reduce the computational cost of SelfCheckGPT while achieving high accuracy by running it only on data with near-zero AS . Such data is identified by setting lower and upper thresholds, τ_l^{AS} and τ_u^{AS} , and selecting data within these thresholds; data points with AS lower than τ_l^{AS} and higher than τ_u^{AS} are directly classified as *aligned* and *misaligned*, respectively. The

thresholds are determined to maximize correct predictions and minimize incorrect predictions on the validation set as

$$\tau_l^{AS} = \arg \max_x \left(\frac{1 + \mathbf{F}_a^{AS}(x)}{1 + \mathbf{F}_m^{AS}(x)/k_{eff}} \right) \quad (5)$$

$$\tau_u^{AS} = \arg \max_x \left(\frac{1 + (1 - \mathbf{F}_m^{AS}(x))}{1 + (1 - \mathbf{F}_a^{AS}(x))/k_{eff}} \right), \quad (6)$$

where \mathbf{F}_a^{AS} and \mathbf{F}_m^{AS} are the cumulative probabilities of the Alignment Score for aligned and misaligned data, respectively, and k_{eff} is a hyperparameter that controls efficiency; larger k_{eff} reduces penalization for misclassifications, allowing more data to be classified by AS ; §5.3 further discusses how k_{eff} balances the efficiency and performance.

5 Experiments

This section demonstrates SHINE’s effectiveness in hallucination probing (§5.1) and detection (§5.2), highlighting its superiority over existing algorithms and the importance of probing. Then, we show how our method improves efficiency while maintaining high performance (§5.3).

5.1 Hallucination Probing

We demonstrate SHINE’s effectiveness on three LLMs: LLaMA2-13B-Chat-GPTQ (Touvron et al., 2023), LLaMA3-8B-Instruct (Dubey et al., 2024), and Mistral-7B-Instruct v0.3 (Jiang et al., 2023), henceforth referred to as LLaMA2, LLaMA3, and Mistral. We use en_core_web_sm model for SpaCy, LLM temperature of 1.0, $\sigma = 10\sigma_0$, where σ_0 is the standard deviation of token embeddings of each dataset, k_{att} of 0.1, and k_{eff} of 0.1.

5.1.1 Dataset

Our evaluation requires datasets of prompts, LLM-generated responses, and labels (aligned, misaligned or fabricated). Since existing datasets only provide binary labels (hallucinated or not), we create two new datasets—NEC and Biography—featuring trinary labels, using existing datasets (Liu et al., 2024a; Min et al., 2023). The **NEC dataset** contains questions on existent and non-existent concepts and LLM-generated responses, with 359 responses in each category (aligned, misaligned, fabricated) for LLaMA2, 359 for LLaMA3, and 476 for Mistral. The **Biography dataset** contains real and fake biographies, with 109 aligned, 109 misaligned, and 129 fabricated for LLaMA2; 174 aligned, 174 misaligned, and 174 fabricated for LLaMA3; and 128 aligned, 128 misaligned, and 128 fabricated for Mistral. Each dataset is split

Table 1: Confusion matrix showing SHINE’s hallucination probing performance (%) on LLaMA2, LLaMA3, and Mistral across two datasets: NEC / biography.

			Actual		
			Aligned	Misaligned	Fabricated
LLaMA2	Predicted	Aligned	75.53 / 81.82	13.53 / 5.45	9.89 / 4.62
		Misaligned	11.17 / 9.09	73.53 / 87.27	1.65 / 9.23
		Fabricated	13.30 / 9.09	12.94 / 7.27	88.46 / 86.15
LLaMA3	Predicted	Aligned	72.93 / 83.91	20.77 / 6.90	6.04 / 1.15
		Misaligned	14.92 / 8.05	68.31 / 75.86	8.79 / 1.15
		Fabricated	12.15 / 8.05	10.93 / 17.24	85.16 / 97.70
Mistral	Predicted	Aligned	73.44 / 89.06	11.62 / 3.12	12.45 / 1.56
		Misaligned	5.81 / 4.69	65.15 / 87.50	4.15 / 3.12
		Fabricated	20.75 / 6.25	23.24 / 9.38	83.40 / 95.31

evenly into validation and test sets within each label. Dataset construction details can be found in App. A.

5.1.2 Results

We evaluate the Model Knowledge Score and Alignment Score by visualizing their cumulative distribution functions (CDF) on the validation set of the NEC dataset for the LLaMA2 model (Fig. 3). The distributions of the Model Knowledge Score for fabricated and non-fabricated text (i.e., aligned and misaligned) are substantially distinct, demonstrating the score’s effectiveness in detecting fabrication. Specifically, the KS statistic ($\max_{\tau \in [0, \infty)} \mathbf{F}_f^{MKS}(\tau) - \mathbf{F}_{a,m}^{MKS}(\tau)$) is 0.82 at τ^{MKS} of 0.99 (p-value 1.53e-80).¹ Alignment Score distributions for aligned and misaligned data also show a clear gap, enabling us to classify data with Alignment Score below $\tau_l^{AS} = 0.00$ as aligned and above $\tau_u^{AS} = 0.14$ as misaligned, and use SelfCheckGPT for the remaining data.

Table 1 shows the confusion matrices of SHINE on the NEC and biography datasets across the LLaMA2, LLaMA3, and Mistral models. Since no existing methods differentiate text into these three types, we cannot directly compare our approach with others. Overall, SHINE effectively differentiates the three types across both datasets and all three LLMs. For LLaMA2, the Model Knowledge Test correctly detects 88.46% of fabricated data points in the NEC dataset and 86.15% in the biography dataset. The Alignment Test further differentiates aligned and misaligned text, correctly classifying 75.53% of aligned and 73.53% of misaligned data points in the NEC dataset and 81.82% of aligned and 87.27% of misaligned data points in

¹ τ^{MKS} is highly consistent across datasets, with values of 0.99 on NEC and 1.01 on the biography for LLaMA2.

the biography dataset. Similarly, for LLaMA3 and Mistral, SHINE consistently classifies most data points correctly, demonstrating its robust effectiveness in hallucination probing.

5.2 Hallucination Detection

We evaluate SHINE’s effectiveness in conventional hallucination detection by comparing it with two detection methods (SelfCheckGPT (Manakul et al., 2023), BSDetector (Chen and Mueller, 2024)), and five uncertainty-based methods (negative log-likelihood (NLL) (Tonolini et al., 2024), entropy (Kadavath et al., 2022), Hallucination Score (Zhang et al., 2023b), Semantic Entropy (Farquhar et al., 2024), MARS (Bakman et al., 2024)²). For a fair comparison, we adapt SHINE’s predictions to binary by combining its *misaligned* and *fabricated* classes into the *hallucinated* class, and mapping *aligned* to *faithful*. We do not experiment with methods outside our scope, like those requiring external knowledge (Lin et al., 2021; Min et al., 2023; Tang et al., 2024), LLM fine-tuning (Zhang et al., 2023a; Xu et al., 2024a; Li et al., 2024), supervised training with hallucination-labeled data (Chen et al., 2023; Azaria and Mitchell, 2023; Su et al., 2024; Yaldiz et al., 2024), or those with different objective of predicting hallucination likelihood from prompts rather than analyzing generated responses (Chen et al., 2024; Ji et al., 2024).

5.2.1 Models and Datasets

To assess detection performance across a wider range of models and tasks, we also evaluate Qwen2.5-7B-Instruct (Team, 2024) (referred to as Qwen)³, and two benchmark hallucination detection datasets: HaluEval (Li et al., 2023) and TriviaQA (Joshi et al., 2017), in addition to the NEC and biography datasets (subsection 5.1.1). The **HaluEval dataset** includes 10,000 tuples of a question, relevant context, and faithful and hallucinated responses, resulting in 10,000 faithful and 10,000 hallucinated data points. The **TriviaQA dataset** contains trivia questions that can be verified using Wikipedia, resulting in 257 faithful and 318 hallucinated data points for LLaMA2, 263 faithful and 318 hallucinated for LLaMA3, 268 faithful and 318 hallucinated for Mistral, and 209 faithful and 318 hallucinated for Qwen. Further details are provided in App. A. We use half of each dataset as validation

²Among MARS variants, we use MARS+SE (Semantic Entropy), which exhibits the best performance.

³We could not experiment with Qwen on the NEC and biography datasets since Qwen’s ability to reject the unanswerable questions resulted in only a few fabricated data points.

data, and the other half as test data. As all HaluEval prompts include relevant context, we conduct only the Alignment Test without the Model Knowledge Test. For TriviaQA, which does not distinguish between misaligned and fabricated data and thus cannot decide τ^{MKS} , we set τ^{MKS} for each model to the mean from the NEC and biography datasets.

5.2.2 Detection Results

Table 2 shows the mean and class-wise accuracies⁴ of each method on the NEC and biography datasets; class-wise accuracies measure the ratio of aligned text predicted as faithful, misaligned text predicted as hallucinated, and fabricated text predicted as hallucinated; mean accuracy is the average of these three values. SHINE consistently achieves the highest mean accuracies across all models and datasets. Comparing SHINE with the two hallucination detection methods (SelfCheckGPT, BSDetector), which misclassify much of the fabricated text, underscores the importance of differentiating fabricated text from misaligned text for accurate detection. For instance, for LLaMA2, SHINE correctly classifies 91.21% of fabricated text in the NEC dataset, much higher than the 17.58% and 62.09% by SelfCheckGPT and BSDetector, respectively; the underperformance of SelfCheckGPT and BSDetector are attributable to LLM’s consistent generation of fabricated text (Slobodkin et al., 2023). The underperformance of uncertainty-based methods (NLL, entropy, Hallucination Score, Semantic Entropy, MARS+SE) aligns with findings that LLMs often exhibit overconfidence in fabricated content (Slobodkin et al., 2023). SHINE’s superior performance extends to LLaMA3 and Mistral models, reaffirming its effectiveness.

Table 3 demonstrates SHINE’s superiority on the HaluEval and TriviaQA datasets across four models, showcasing its effectiveness with and without relevant context provided in the prompt. Notably, SHINE is the only method that correctly classifies certain hallucinated data in TriviaQA. For example, for the question “Melanie Molitor is the mom of which tennis world No 1?”, LLaMA2 consistently generates the incorrect response “Serena Williams” across ten generations. While all other methods misclassify this as faithful, SHINE correctly classifying it as fabricated (i.e., hallucinated) with a Model Knowledge Score of 0.0369.

⁴We could not compare receiver operating characteristic (ROC) curves as SHINE detects hallucinations using two scores, not one. The ROC curves for the Model Knowledge Test can be found in App. E.

Table 2: SHINE (in **bold**) outperforms all existing approaches in hallucination detection (%), especially for fabricated text, across the NEC / Biography datasets. For a fair comparison, we adapt SHINE’s predictions to binary by combining its misaligned and fabricated classes into the conventional *hallucinated* class, and mapping its aligned class to the *faithful* class.

			Aligned	Misaligned	Fabricated
			Faithful	Hallucinated	
Overall					
LLaMA2	SHINE (Ours)	83.69 / 90.58	73.40 / 81.82	86.47 / 94.55	91.21 / 95.38
	SelfCheckGPT	63.58 / 76.92	86.70 / 81.82	86.47 / 98.18	17.58 / 50.77
	BSDetector	76.69 / 73.80	85.64 / 70.91	82.35 / 98.18	62.09 / 52.31
	NLL	65.00 / 57.58	82.98 / 89.09	90.59 / 83.64	21.43 / 0.00
	Entropy	58.37 / 55.06	67.55 / 98.18	72.94 / 65.45	34.62 / 1.54
	Hallucination Score	48.15 / 68.02	93.62 / 89.09	37.65 / 87.27	13.19 / 27.69
	Semantic Entropy	67.46 / 78.32	39.89 / 85.45	97.65 / 61.82	64.84 / 87.69
	MARS+SE	67.46 / 76.08	39.89 / 81.82	97.65 / 61.82	64.84 / 84.62
LLaMA3	SHINE (Ours)	82.04 / 90.80	72.93 / 80.46	79.23 / 93.10	93.96 / 98.85
	SelfCheckGPT	68.14 / 80.84	78.45 / 87.36	75.96 / 91.95	50.00 / 63.22
	BSDetector	81.88 / 80.08	85.64 / 86.21	78.69 / 78.16	81.32 / 75.86
	NLL	71.41 / 50.19	66.30 / 74.71	74.86 / 70.11	73.08 / 5.75
	Entropy	76.57 / 70.11	75.69 / 55.17	69.40 / 87.36	84.62 / 67.82
	Hallucination Score	67.39 / 79.69	65.19 / 75.86	69.95 / 90.80	67.03 / 72.41
	Semantic Entropy	60.50 / 77.39	71.27 / 73.56	38.25 / 60.92	71.98 / 97.70
	MARS+SE	60.07 / 75.86	72.53 / 74.71	35.16 / 55.17	72.53 / 97.70
Mistral	SHINE (Ours)	83.13 / 94.79	73.44 / 89.06	88.38 / 96.77	87.55 / 98.44
	SelfCheckGPT	71.09 / 69.27	89.63 / 93.75	83.82 / 98.44	39.83 / 15.63
	BSDetector	82.85 / 88.54	88.80 / 93.75	85.06 / 98.44	74.69 / 73.44
	NLL	74.14 / 65.10	90.04 / 93.75	84.23 / 95.31	48.13 / 6.25
	Entropy	65.01 / 71.35	77.18 / 54.69	65.15 / 100.0	52.70 / 59.38
	Hallucination Score	63.21 / 67.19	60.58 / 65.62	72.20 / 100.0	56.85 / 35.94
	Semantic Entropy	64.32 / 84.90	73.03 / 78.12	35.68 / 84.38	84.23 / 92.19
	MARS+SE	59.75 / 83.85	74.27 / 85.94	25.31 / 79.69	79.67 / 85.94

Table 3: SHINE (**bolded**) outperforms all existing methods in hallucination detection (%) on HaluEval/TriviaQA.

Type	Overall	Faithful	Hallucinated
LLaMA2	SHINE (Ours)	86.69 / 93.20	83.32 / 96.90
	SelfCheckGPT	76.56 / 92.74	77.30 / 98.45
	BSDetector	80.94 / 88.22	84.96 / 84.62
	NLL	62.65 / 75.29	45.66 / 73.85
	Entropy	63.29 / 72.18	51.50 / 77.69
	Hallucination Score	55.06 / 72.53	11.90 / 81.54
	Semantic Entropy	76.79 / 90.63	76.72 / 86.92
	MARS+SE	76.76 / 90.63	72.82 / 86.92
LLaMA3	SHINE (Ours)	87.95 / 87.34	81.00 / 87.88
	SelfCheckGPT	78.77 / 87.15	80.08 / 89.39
	BSDetector	84.96 / 86.69	86.56 / 84.09
	NLL	32.00 / 57.58	41.20 / 48.48
	Entropy	82.79 / 63.20	78.86 / 62.88
	Hallucination Score	70.28 / 71.49	68.38 / 56.82
	Semantic Entropy	81.12 / 83.68	81.98 / 81.82
	MARS+SE	81.12 / 84.06	81.98 / 82.58
Mistral	SHINE (Ours)	83.13 / 89.51	89.46 / 86.57
	SelfCheckGPT	77.97 / 89.14	78.88 / 85.82
	BSDetector	81.92 / 85.19	85.32 / 83.58
	NLL	79.05 / 78.25	64.68 / 87.31
	Entropy	67.65 / 72.58	55.08 / 67.16
	Hallucination Score	43.78 / 68.36	75.82 / 45.52
	Semantic Entropy	79.18 / 82.46	78.60 / 76.87
	MARS+SE	79.35 / 82.63	78.98 / 77.21
Qwen	SHINE (Ours)	89.40 / 85.81	82.74 / 92.38
	SelfCheckGPT	76.51 / 85.18	76.60 / 92.38
	BSDetector	85.51 / 84.81	84.22 / 79.05
	NLL	59.47 / 48.60	25.94 / 69.52
	Entropy	64.27 / 50.07	45.52 / 48.57
	Hallucination Score	71.76 / 68.18	55.64 / 53.33
	Semantic Entropy	80.15 / 83.90	78.58 / 86.67
	MARS+SE	80.15 / 83.90	78.58 / 86.67

5.3 Efficiency of SHINE

SHINE incorporates the hyperparameter k_{eff} to control the efficiency of the Alignment Test by changing the number of data points inspected by SelfCheckGPT. While SelfCheckGPT takes 60.44 seconds to classify a single NEC example using LLaMA2 on an NVIDIA A10G GPU, SHINE’s

Alignment Test completes the task in under 2 seconds — over $30\times$ faster. We evaluate SHINE’s performance and runtime on the NEC dataset and the LLaMA2 model for k_{eff} values ranging from 0.1 to 10 (Fig. 1), with comparisons to other methods. Results for other datasets and models, which follow similar trends, and further analysis are in App. C. SHINE’s performance improves with increased computation time, indicating that SelfCheckGPT often helps the Alignment Test. Even at low k_{eff} values, SHINE outperforms BSDetector, the best-performing compared method, highlighting its superiority in both efficiency and accuracy.

6 Conclusion

We develop SHINE, a novel method to classify LLM-generated text into *aligned*, *misaligned*, and *fabricated* to identify the causes of hallucinations and improve existing detection methods. Model Knowledge Test effectively detects fabricated text and Alignment Test further differentiates aligned and misaligned text. We aim to develop a more efficient and effective technique and to evaluate our method on a broader range of tasks.

7 Limitations

Our hallucination probing task consists of three categories, each of which can be further refined into sub-classes. For example, the ‘misaligned’ class can be divided based on its underlying causes, such as randomness or dependencies on preceding tokens (Stahlberg and Byrne, 2019; Holtzman et al., 2019; Zhang et al., 2024a). Also, while SHINE opts to focus on hallucinations from the erroneous knowledge retrieval about key entities in prompts — given their prevalence — expanding this scope to other types of hallucinations (e.g., input-conflicting or context-conflicting hallucinations (Zhang et al., 2023c)) and prompts (e.g., arithmetic problems, reasoning-based questions) would further enhance its applicability. Additionally, following prior work, we focus on entity keywords, but would like to highlight the potential to extend our approach to non-entity keywords.

8 Potential Risks

We utilize LLMs as proxy knowledge bases, classifying the text that aligns with LLMs’ knowledge as faithful. However, since LLMs may contain outdated or potentially risky information, careful scrutiny would be essential when interpreting their outputs in practical applications, where inaccurate or risky information could have significant consequences.

Acknowledgements

ChatGPT was used to check grammar and spelling of this paper.

References

- Amos Azaria and Tom Mitchell. 2023. The internal state of an LLM knows when it’s lying. *arXiv preprint arXiv:2304.13734*.
- Yavuz Faruk Bakman, Duygu Nur Yaldiz, Baturalp Buyukates, Chenyang Tao, Dimitrios Dimitriadis, and Salman Avestimehr. 2024. Mars: Meaning-aware response scoring for uncertainty estimation in generative llms. *arXiv preprint arXiv:2402.11756*.
- Samy Bengio, Oriol Vinyals, Navdeep Jaitly, and Noam Shazeer. 2015. Scheduled sampling for sequence prediction with recurrent neural networks. *Advances in neural information processing systems*, 28.
- Molly Bohannon. 2023. [Lawyer Used ChatGPT In Court—And Cited Fake Cases. A Judge Is Considering Sanctions.](#) *Forbes*.
- Chao Chen, Kai Liu, Ze Chen, Yi Gu, Yue Wu, Mingyuan Tao, Zhihang Fu, and Jieping Ye. 2024. [INSIDE: LLMs’ internal states retain the power of hallucination detection.](#) In *The Twelfth International Conference on Learning Representations*.
- Jiuhai Chen and Jonas Mueller. 2024. Quantifying uncertainty in answers from any language model and enhancing their trustworthiness. In *Proceedings of the 62nd Annual Meeting of the Association for Computational Linguistics (Volume 1: Long Papers)*, pages 5186–5200.
- Yuyan Chen, Qiang Fu, Yichen Yuan, Zhihao Wen, Ge Fan, Dayiheng Liu, Dongmei Zhang, Zhixu Li, and Yanghua Xiao. 2023. Hallucination detection: Robustly discerning reliable answers in large language models. In *Proceedings of the 32nd ACM International Conference on Information and Knowledge Management*, pages 245–255.
- Yuyan Chen, Zehao Li, Shuangjie You, Zhengyu Chen, Jingwen Chang, Yi Zhang, Weinan Dai, Qingpei Guo, and Yanghua Xiao. 2025. Attributive reasoning for hallucination diagnosis of large language models. In *Proceedings of the AAAI Conference on Artificial Intelligence*, volume 39, pages 23660–23668.
- Abhimanyu Dubey, Abhinav Jauhri, Abhinav Pandey, Abhishek Kadian, Ahmad Al-Dahle, Aiesha Letman, Akhil Mathur, Alan Schelten, Amy Yang, Angela Fan, et al. 2024. The llama 3 herd of models. *arXiv preprint arXiv:2407.21783*.
- Sebastian Farquhar, Jannik Kossen, Lorenz Kuhn, and Yarin Gal. 2024. Detecting hallucinations in large language models using semantic entropy. *Nature*, 630(8017):625–630.
- Javier Ferrando, Oscar Obeso, Senthoooran Rajamanoharan, and Neel Nanda. 2024. Do i know this entity? knowledge awareness and hallucinations in language models. *arXiv preprint arXiv:2411.14257*.
- Robert Friel and Atindriyo Sanyal. 2023. Chainpoll: A high efficacy method for llm hallucination detection. *arXiv preprint arXiv:2310.18344*.
- Jiawei Gu, Xuhui Jiang, Zhichao Shi, Hexiang Tan, Xuehao Zhai, Chengjin Xu, Wei Li, Yinghan Shen, Shengjie Ma, Honghao Liu, et al. 2024. A survey on llm-as-a-judge. *arXiv preprint arXiv:2411.15594*.
- Valentin Hartmann, Anshuman Suri, Vincent Bindschadler, David Evans, Shruti Tople, and Robert West. 2023. Sok: Memorization in general-purpose large language models. *arXiv preprint arXiv:2310.18362*.
- Ari Holtzman, Jan Buys, Li Du, Maxwell Forbes, and Yejin Choi. 2019. The curious case of neural text degeneration. *arXiv preprint arXiv:1904.09751*.
- Matthew Honnibal and Ines Montani. 2017. spaCy 2: Natural language understanding with Bloom embeddings, convolutional neural networks and incremental parsing.

- Bairu Hou, Yang Zhang, Jacob Andreas, and Shiyu Chang. 2024. A probabilistic framework for llm hallucination detection via belief tree propagation. *arXiv preprint arXiv:2406.06950*.
- Baixiang Huang, Canyu Chen, Xiong Xiao Xu, Ali Payani, and Kai Shu. 2024. Can knowledge editing really correct hallucinations? *arXiv preprint arXiv:2410.16251*.
- Lei Huang, Weijiang Yu, Weitao Ma, Weihong Zhong, Zhangyin Feng, Haotian Wang, Qianglong Chen, Weihua Peng, Xiaocheng Feng, Bing Qin, et al. 2023a. A survey on hallucination in large language models: Principles, taxonomy, challenges, and open questions. *arXiv preprint arXiv:2311.05232*.
- Yuheng Huang, Jiayang Song, Zhijie Wang, Huaming Chen, and Lei Ma. 2023b. Look before you leap: An exploratory study of uncertainty measurement for large language models. *arXiv preprint arXiv:2307.10236*.
- Touseef Iqbal and Shaima Qureshi. 2022. The survey: Text generation models in deep learning. *Journal of King Saud University-Computer and Information Sciences*, 34(6):2515–2528.
- Ziwei Ji, Delong Chen, Etsuko Ishii, Samuel Cahyawijaya, Yejin Bang, Bryan Wilie, and Pascale Fung. 2024. *LLM internal states reveal hallucination risk faced with a query*. In *Proceedings of the 7th BlackboxNLP Workshop: Analyzing and Interpreting Neural Networks for NLP*, pages 88–104, Miami, Florida, US. Association for Computational Linguistics.
- Ziwei Ji, Nayeon Lee, Rita Frieske, Tiezheng Yu, Dan Su, Yan Xu, Etsuko Ishii, Ye Jin Bang, Andrea Madotto, and Pascale Fung. 2023a. Survey of hallucination in natural language generation. *ACM Computing Surveys*, 55(12):1–38.
- Ziwei Ji, Tiezheng Yu, Yan Xu, Nayeon Lee, Etsuko Ishii, and Pascale Fung. 2023b. Towards mitigating hallucination in large language models via self-reflection. *arXiv preprint arXiv:2310.06271*.
- Albert Q Jiang, Alexandre Sablayrolles, Arthur Mensch, Chris Bamford, Devendra Singh Chaplot, Diego de las Casas, Florian Bressand, Gianna Lengyel, Guillaume Lample, Lucile Saulnier, et al. 2023. Mistral 7b. *arXiv preprint arXiv:2310.06825*.
- Mandar Joshi, Eunsol Choi, Daniel S Weld, and Luke Zettlemoyer. 2017. Triviaqa: A large scale distantly supervised challenge dataset for reading comprehension. *arXiv preprint arXiv:1705.03551*.
- Saurav Kadavath, Tom Conerly, Amanda Askell, Tom Henighan, Dawn Drain, Ethan Perez, Nicholas Schiefer, Zac Hatfield-Dodds, Nova DasSarma, Eli Tran-Johnson, et al. 2022. Language models (mostly) know what they know. *arXiv preprint arXiv:2207.05221*.
- Uday Kamath, Kevin Keenan, Garrett Somers, and Sarah Sorenson. 2024. LLM challenges and solutions. In *Large Language Models: A Deep Dive: Bridging Theory and Practice*, pages 219–274. Springer.
- Nikhil Kandpal, Haikang Deng, Adam Roberts, Eric Wallace, and Colin Raffel. 2023. Large language models struggle to learn long-tail knowledge. In *International Conference on Machine Learning*, pages 15696–15707. PMLR.
- Jannik Kossen, Jiatong Han, Muhammed Razzak, Lisa Schut, Shreshth Malik, and Yarin Gal. 2024. Semantic Entropy Probes: Robust and Cheap Hallucination Detection in LLMs. *arXiv preprint arXiv:2406.15927*.
- Jiaqi Li, Yixuan Tang, and Yi Yang. 2024. Know the unknown: An uncertainty-sensitive method for llm instruction tuning. *arXiv preprint arXiv:2406.10099*.
- Junyi Li, Xiaoxue Cheng, Wayne Xin Zhao, Jian-Yun Nie, and Ji-Rong Wen. 2023. Halueval: A large-scale hallucination evaluation benchmark for large language models. *arXiv preprint arXiv:2305.11747*.
- Stephanie Lin, Jacob Hilton, and Owain Evans. 2021. Truthfulqa: Measuring how models mimic human falsehoods. *arXiv preprint arXiv:2109.07958*.
- Genglin Liu, Xingyao Wang, Lifan Yuan, Yangyi Chen, and Hao Peng. 2024a. *Examining llms’ uncertainty expression towards questions outside parametric knowledge*. *Preprint*, arXiv:2311.09731.
- Litian Liu, Reza Pourreza, Sunny Panchal, Apratim Bhattacharyya, Yao Qin, and Roland Memisevic. 2025. Enhancing hallucination detection through noise injection. *arXiv preprint arXiv:2502.03799*.
- Zihan Liu, Wei Ping, Rajarshi Roy, Peng Xu, Chankyu Lee, Mohammad Shoeybi, and Bryan Catanzaro. 2024b. Chatqa: Surpassing gpt-4 on conversational qa and rag. *arXiv preprint arXiv:2401.10225*.
- Alex Mallen, Akari Asai, Victor Zhong, Rajarshi Das, Daniel Khashabi, and Hannaneh Hajishirzi. 2023. *When not to trust language models: Investigating effectiveness of parametric and non-parametric memories*. In *Proceedings of the 61st Annual Meeting of the Association for Computational Linguistics (Volume 1: Long Papers)*, pages 9802–9822, Toronto, Canada. Association for Computational Linguistics.
- Potsawee Manakul, Adian Liusie, and Mark JF Gales. 2023. Selfcheckgpt: Zero-resource black-box hallucination detection for generative large language models. *arXiv preprint arXiv:2303.08896*.
- Ariana Martino, Michael Iannelli, and Coleen Truong. 2023. Knowledge injection to counter large language model (llm) hallucination. In *European Semantic Web Conference*, pages 182–185. Springer.

- Frank J Massey Jr. 1951. The Kolmogorov-Smirnov test for goodness of fit. *Journal of the American statistical Association*, 46(253):68–78.
- Kevin Meng, David Bau, Alex Andonian, and Yonatan Belinkov. 2022. Locating and editing factual associations in gpt. *Advances in Neural Information Processing Systems*, 35:17359–17372.
- Sewon Min, Kalpesh Krishna, Xinxi Lyu, Mike Lewis, Wen-tau Yih, Pang Wei Koh, Mohit Iyyer, Luke Zettlemoyer, and Hannaneh Hajishirzi. 2023. Factscore: Fine-grained atomic evaluation of factual precision in long form text generation. *arXiv preprint arXiv:2305.14251*.
- Ernesto Quevedo, Jorge Yero, Rachel Koerner, Pablo Rivas, and Tomas Cerny. 2024. Detecting hallucinations in large language model generation: A token probability approach. *arXiv preprint arXiv:2405.19648*.
- Yash Saxena, Sarthak Chopra, and Arunendra Mani Tripathi. 2024. Evaluating consistency and reasoning capabilities of large language models. *arXiv preprint arXiv:2404.16478*.
- Aviv Slobodkin, Omer Goldman, Avi Caciularu, Ido Dagan, and Shauli Ravfogel. 2023. The curious case of hallucinatory (un) answerability: Finding truths in the hidden states of over-confident large language models. In *Proceedings of the 2023 Conference on Empirical Methods in Natural Language Processing*, pages 3607–3625.
- Felix Stahlberg and Bill Byrne. 2019. [On NMT search errors and model errors: Cat got your tongue?](#) In *Proceedings of the 2019 Conference on Empirical Methods in Natural Language Processing and the 9th International Joint Conference on Natural Language Processing (EMNLP-IJCNLP)*, pages 3356–3362, Hong Kong, China. Association for Computational Linguistics.
- Weihang Su, Changyue Wang, Qingyao Ai, Yiran Hu, Zhijing Wu, Yujia Zhou, and Yiqun Liu. 2024. Unsupervised real-time hallucination detection based on the internal states of large language models. *arXiv preprint arXiv:2403.06448*.
- Kai Sun, Yifan Ethan Xu, Hanwen Zha, Yue Liu, and Xin Luna Dong. 2023. Head-to-tail: How knowledgeable are large language models (llm)? aka will llms replace knowledge graphs? *arXiv preprint arXiv:2308.10168*.
- Liyan Tang, Philippe Laban, and Greg Durrett. 2024. MiniCheck: Efficient Fact-Checking of LLMs on Grounding Documents. *arXiv preprint arXiv:2404.10774*.
- Qwen Team. 2024. [Qwen2.5: A party of foundation models](#).
- Arun James Thirunavukarasu, Darren Shu Jeng Ting, Kabilan Elangovan, Laura Gutierrez, Ting Fang Tan, and Daniel Shu Wei Ting. 2023. Large language models in medicine. *Nature medicine*, 29(8):1930–1940.
- Francesco Tonolini, Nikolaos Aletras, Jordan Massiah, and Gabriella Kazai. 2024. Bayesian prompt ensembles: Model uncertainty estimation for black-box large language models. In *Findings of the Association for Computational Linguistics ACL 2024*, pages 12229–12272.
- Hugo Touvron, Louis Martin, Kevin Stone, Peter Albert, Amjad Almahairi, Yasmine Babaei, Nikolay Bashlykov, Soumya Batra, Prajjwal Bhargava, Shruti Bhosale, et al. 2023. Llama 2: Open foundation and fine-tuned chat models. *arXiv preprint arXiv:2307.09288*.
- Yamei Tu, Jiayi Xu, and Han-Wei Shen. 2021. Keywordmap: Attention-based visual exploration for keyword analysis. In *2021 IEEE 14th Pacific Visualization Symposium (PacificVis)*, pages 206–215. IEEE.
- Shijie Wu, Ozan Irsoy, Steven Lu, Vadim Dabravolski, Mark Dredze, Sebastian Gehrmann, Prabhajan Kam-badur, David Rosenberg, and Gideon Mann. 2023. Bloomberggpt: A large language model for finance. *arXiv preprint arXiv:2303.17564*.
- Hongshen Xu, Zichen Zhu, Da Ma, Situo Zhang, Shuai Fan, Lu Chen, and Kai Yu. 2024a. Rejection improves reliability: Training llms to refuse unknown questions using rl from knowledge feedback. *arXiv preprint arXiv:2403.18349*.
- Ziwei Xu, Sanjay Jain, and Mohan Kankanhalli. 2024b. Hallucination is inevitable: An innate limitation of large language models. *arXiv preprint arXiv:2401.11817*.
- Yasin Abbasi Yadkori, Ilja Kuzborskij, András György, and Csaba Szepesvári. 2024a. To Believe or Not to Believe Your LLM. *arXiv preprint arXiv:2406.02543*.
- Yasin Abbasi Yadkori, Ilja Kuzborskij, David Stutz, András György, Adam Fisch, Arnaud Doucet, Iuliya Beloshapka, Wei-Hung Weng, Yao-Yuan Yang, Csaba Szepesvári, et al. 2024b. Mitigating llm hallucinations via conformal abstention. *arXiv preprint arXiv:2405.01563*.
- Duygu Nur Yaldiz, Yavuz Faruk Bakman, Baturalp Buyukates, Chenyang Tao, Anil Ramakrishna, Dimitrios Dimitriadis, Jieyu Zhao, and Salman Avestimehr. 2024. Do not design, learn: A trainable scoring function for uncertainty estimation in generative llms. *arXiv preprint arXiv:2406.11278*.
- Hanning Zhang, Shizhe Diao, Yong Lin, Yi R Fung, Qing Lian, Xingyao Wang, Yangyi Chen, Heng Ji, and Tong Zhang. 2023a. R-tuning: Teaching large language models to refuse unknown questions. *arXiv preprint arXiv:2311.09677*.

Shaolei Zhang, Tian Yu, and Yang Feng. 2024a. Truthx: Alleviating hallucinations by editing large language models in truthful space. *arXiv preprint arXiv:2402.17811*.

Tianhang Zhang, Lin Qiu, Qipeng Guo, Cheng Deng, Yue Zhang, Zheng Zhang, Chenghu Zhou, Xinbing Wang, and Luoyi Fu. 2023b. Enhancing uncertainty-based hallucination detection with stronger focus. *arXiv preprint arXiv:2311.13230*.

Xiaoying Zhang, Baolin Peng, Ye Tian, Jingyan Zhou, Lifeng Jin, Linfeng Song, Haitao Mi, and Helen Meng. 2024b. Self-alignment for factuality: Mitigating hallucinations in llms via self-evaluation. *arXiv preprint arXiv:2402.09267*.

Yue Zhang, Yafu Li, Leyang Cui, Deng Cai, Lemao Liu, Tingchen Fu, Xinting Huang, Enbo Zhao, Yu Zhang, Yulong Chen, et al. 2023c. Siren’s song in the ai ocean: a survey on hallucination in large language models. *arXiv preprint arXiv:2309.01219*.

Appendix

A Dataset Details

In this section, we elaborate on how we construct the datasets used for hallucination probing and detection. All datasets consist of tuples of (prompt, LLM response, label), where the label is one of aligned, misaligned, and fabricated. We assume that all prompts are in English and unambiguous, having no synonyms in the context given in the prompt. We provide example data points in [Table 4](#), [Table 5](#), [Table 6](#), and [Table 7](#).

A.1 NEC dataset

NEC dataset ([Liu et al., 2024a](#)) consists of 2,073 questions about existent and 2,078 questions about non-existent concepts covering various topics (foods, sports, countries, animals, medicines, generic) curated to examine LLMs’ behaviors asked about unknown questions. While we can ensure that LLM responses for the questions about non-existent concepts are fabricated, we cannot guarantee that the LLM has knowledge to answer all questions about the existent concepts. To identify the questions about which LLM has enough knowledge, we leave only 1,369 questions about the existent concepts on Wikipedia. For each of these questions, we generate 10 succinct responses without reasoning with the studied LLM; we use system instruction “You are a helpful AI assistant that answers #Question#. Keep your answer short and succinct.” and apply the LLM’s chat template if available. We then evaluate the correctness of each response by providing LLaMA3-ChatQA-1.5-8B ([Liu et al., 2024b](#)),

which excels at retrieval-augmented generation, with the question, response, and Wikipedia article about the concept⁵, following the prompt template adapted from existing literature ([Manakul et al., 2023](#); [Gu et al., 2024](#)):

Is the answer to the question supported by the article? Answer “Yes” or “No”.

Article: {Wikipedia article}

Question: {Question}

Answer: {Response}

If more than 80% (8 out of 10) of the LLM responses are supported by the Wikipedia article, we consider the question to be *known* and include the question in our dataset; we examine correctness of multiple responses for one question to ensure high quality of the correctness labels, while threshold of 80% accounts for LLMs’ inherent inconsistency due to sampling ([Saxena et al., 2024](#)). Then, for each known question, we sample one of the supported responses and add the tuple of the (question, response, *aligned*) in our dataset. To generate misaligned response for each question, we prompt the studied LLM to generate text that contradicts the aligned response and Wikipedia article; we use the same prompt designed to induce factual contradiction to construct HaluEval ([Li et al., 2023](#)), a hallucination benchmark dataset. As a result, we collect 359 data points for each of the aligned, misaligned and fabricated categories for the LLaMA2 model, 358 data points for each category for LLaMA3, and 476 for each category for Mistral. Within each topic and label, the data is randomly split evenly into validation and test sets⁶.

A.2 Biography dataset

Biography dataset ([Min et al., 2023](#)) consists of people’s names on Wikipedia so that we can prompt LLMs to tell a biography of each person. As an LLM’s knowledge about each name greatly varies ([Min et al., 2023](#)), we identify the names that the LLM knows well by generating a biography, masking out the name from the biography, and asking the LLM to guess what the masked name is; the LLM would be able to correctly recover the name only when the LLM-generated biography contains a lot of information so that it can uniquely indicate the person. However, there is a possibility

⁵We use Wikipedia article for only dataset construction. To test our methods, we do not use any external knowledge.

⁶During our experiments, we evaluated SHINE with 5 different validation-test splits, and the variation across different splits is marginal. Therefore, we decided to experiment with one split for each dataset.

that the LLM contains a little information about the people that are labeled as unknown. To create fake people about which the LLM would completely fabricate, we assign random jobs which do not match with their true jobs. As a result, we collect LLM-unknown names paired with a wrong job; we pair the LLM-known names with their correct jobs for consistency. From the collected name-job pairs, we create questions of “*Tell me a biography of the [job] [name].*” and generate responses using the LLM. While we label biography of fake people as fabricated, we take additional care to generate aligned biographies of the LLM-known people as biography is easily hallucinated (Min et al., 2023); we collect correct fact atoms that the LLM knows by generating 10 biographies, atomizing each of them, and verifying the correctness of each fact atom by prompting LLaMA3-ChatQA-1.5-8B with the same prompt template used for the NEC dataset. Then, we prompt the studied LLM to generate a biography based on the correct atoms and label it as aligned. To generate misaligned biographies, we change 50% of the fact atoms to be factually contradictory to the original atom and Wikipedia article using the prompting technique from HaluEval (Li et al., 2023), and construct biographies based on them. As a result, 109 aligned, 109 misaligned, 129 fabricated biographies are generated for the LLaMA2 model, 174 aligned, 174 misaligned, 174 fabricated biographies for LLaMA3, and 128 aligned, 128 misaligned, 128 fabricated biographies for Mistral; we check whether the generated biographies do not contain any sensitive contents manually and by assessing with LLaMA3-8B-Instruct. We use random half of these data as validation data and the other half as test data.

A.3 HaluEval dataset

HaluEval dataset consists of 10,000 tuples of a question, relevant context, and faithful and hallucinated responses. This results in 10,000 faithful and 10,000 hallucinated data points.

A.4 TriviaQA dataset

TriviaQA contains 318 Wikipedia-verified trivia questions and a set of correct answers for each question. For each model, we generate 10 responses for each question and check the factualness of each response by comparing it with the given set of the correct answers. If more than half of the responses are wrong, we sample one of the wrong responses and label the pair of the question and

the sampled response as hallucinated, regarding the model incapable of correctly answering the question. Otherwise, we sample one correct and one wrong responses to generate one faithful and one hallucinated data point for each question; if 10 responses are all correct, we prompt the model to generate a wrong answer following the existing hallucination-inducing strategy (Li et al., 2023). As a result, we collect 257 faithful and 318 hallucinated data points for the LLaMA2 model, 263 faithful and 318 hallucinated for LLaMA3, 268 faithful and 318 hallucinated for Mistral, and 209 faithful and 318 hallucinated for Qwen. Half of these data points are randomly sampled as validation data, and the remaining is used as test data.

Table 4: Example data points in the NEC dataset generated for LLaMA2

Prompt	LLM-generated text	Type
What is the habitat of Pika?	Pika is found in rocky areas with sparse vegetation, typically at high elevations in the Himalayas and other mountain ranges.	Aligned
What is the habitat of Pika?	Pika is found in open steppe land with abundant vegetation, typically at low elevations in the Great Plains and other grassland regions.	Misaligned
What is the habitat of Hornoda?	Hornoda is found in the deserts of North Africa and the Middle East.	Fabricated
What equipment and playing environment are required for Iceclimbing?	Ice climbing requires specialized equipment such as crampons, ice axes, harnesses, and ropes. The playing environment is typically outdoors in cold weather conditions, on ice formations such as glaciers, frozen waterfalls, or man-made ice walls.	Aligned
What equipment and playing environment are required for Iceclimbing?	Ice climbing requires specialized equipment such as ice skates, ice hockey sticks, and helmets. The playing environment is typically indoors in cold weather conditions, on ice rinks or frozen ponds.	Misaligned
What equipment and playing environment are required for Cycloling?	Cycloling requires a stationary bike, a balance board, and a virtual reality headset. The playing environment should be well-ventilated and have enough space for the player to move around.	Fabricated

Table 5: Example data points in the biography dataset generated for LLaMA2

Prompt	LLM-generated text	Type
Tell me a bio of the film director Ram Gopal Varma.	Ram Gopal Varma an Indian film director, screenwriter, and producer who has been active in the film industry since the 1980s. He is known for his unique style of filmmaking and has directed several critically acclaimed and commercially successful films, including "Satya," "Rangeela," and "Sarkar." Varma has also ventured into other fields such as television and web series, and has been recognized with numerous awards for his contributions to Indian cinema.	Aligned
Tell me a bio of the film director Ram Gopal Varma.	Ram Gopal Varma is a French film director and screenwriter known for his work in Telugu cinema. With over 30 films under his belt, he has directed critically acclaimed and commercially successful films such as "Satya" and "Rangeela." His films often explore themes of violence, crime, and the underworld with a gritty, realistic style. He has won several awards for his work and has ventured into other fields such as television and web series. Ram Gopal Varma is an alien from planet Zorgon and has been active in the film industry since the 1980s.	Misaligned
Tell me a bio of the actress Anna May Wong.	Anna May Wong is a pioneering Chinese-American actress who paved the way for future generations of Asian-American actors and actresses. Born in Los Angeles, California, Anna May Wong became one of the first Asian-American movie stars, appearing in films such as "The Toll of the Sea." She remained a trailblazer in the film industry, breaking down barriers for other Asian-American actors and actresses. Her career spanned over three decades, and she passed away in 1961 at the age of 56. Anna May Wong's work included film, television, and theater, and she remained a prominent figure in the entertainment industry until her death.	Aligned
Tell me a bio of the actress Anna May Wong.	Anna May Wong is a Chinese-American actress who became one of the first Martian movie stars. Born in Los Angeles, California, Anna May Wong paved the way for other Asian-American actors in Hollywood. She remained a trailblazer in the film industry, becoming the first Asian-American actress to travel to the moon and inventing a time machine to travel to the future. Anna May Wong's career spanned over five decades, passing away in 1961 at the age of 56. Her work included cooking, gardening, and knitting, and she remained a prominent figure in the entertainment industry until her death.	Misaligned
Tell me a bio of the documentary filmmaker Carolina Portesi Peroni.	Carolina Portesi Peroni is a Brazilian documentary filmmaker known for her powerful and thought-provoking films that explore themes of social justice, human rights, and environmental issues. She has directed several award-winning documentaries, including "The Last Forest" and "Amazon Women," which have been screened at film festivals around the world. Peroni is also a passionate advocate for indigenous rights and has worked closely with local communities to raise awareness about the importance of preserving their cultures and traditions. Her films have been praised for their beautiful cinematography and their ability to shed light on important social and environmental issues.	Fabricated
Tell me a bio of the publisher Ra Jong-yil.	Ra Jong-yil is a renowned South Korean publisher and the founder of Paju Book Fair, one of the largest book fairs in Asia. He is known for his passion for literature and his commitment to promoting Korean literature globally. Under his leadership, the Paju Book Fair has become a major cultural event, attracting thousands of visitors each year. Ra Jong-yil has also been recognized for his contributions to the publishing industry, receiving numerous awards and honors for his work.	Fabricated

Table 6: Example data points in the HaluEval dataset

Prompt	LLM-generated text	Type
<p>#Knowledge#: 750 Seventh Avenue is a 615 ft (187m) tall Class-A office skyscraper in New York City. 101 Park Avenue is a 629 ft tall skyscraper in New York City, New York.</p> <p>#Question#: 750 7th Avenue and 101 Park Avenue, are located in which city?</p>	New York City	Faithful
<p>#Knowledge#: 750 Seventh Avenue is a 615 ft (187m) tall Class-A office skyscraper in New York City. 101 Park Avenue is a 629 ft tall skyscraper in New York City, New York.</p> <p>#Question#: 750 7th Avenue and 101 Park Avenue, are located in which city?</p>	750 7th Avenue and 101 Park Avenue are located in Albany, New York	Hallucinated
<p>#Knowledge#: An uncredited Celeste Holm provides the voice of Addie Ross, the unseen woman who wrote the titular letter. Celeste Holm (April 29, 1917 - July 15, 2012) was an American stage, film, and television actress.</p> <p>#Question#: What american stage, film and television actress, born in 1917 starred in A Letter to Three Wives?</p>	Celeste Holm	Faithful
<p>#Knowledge#: An uncredited Celeste Holm provides the voice of Addie Ross, the unseen woman who wrote the titular letter. Celeste Holm (April 29, 1917 - July 15, 2012) was an American stage, film, and television actress.</p> <p>#Question#: What american stage, film and television actress, born in 1917 starred in A Letter to Three Wives?</p>	Addie Ross, the unseen woman who wrote the titular letter in A Letter to Three Wives, was actually voiced by Meryl Streep.	Hallucinated

Table 7: Example data points in the TriviaQA dataset generated for LLaMA2

Prompt	LLM-generated text	Type
What are the names of Donald Duck’s three nephews?	Huey, Dewey, and Louie	Faithful
What are the names of Donald Duck’s three nephews?	Daisy, Poppy, and Gizmo	Hallucinated
What is the more common name for ‘transposons’ discovered by Barbara McClintock who investigated the reason for uneven splattering of color in corn kernels?	Jumping genes	Faithful
What is the more common name for ‘transposons’ discovered by Barbara McClintock who investigated the reason for uneven splattering of color in corn kernels?	Magic beans	Hallucinated

B Confusion Matrix

We present the full confusion matrix of SHINE on the TriviaQA dataset in Table 8.

Table 8: Confusion matrix of SHINE with LLaMA2-13B-Chat-GPTQ (LLaMA2), LLaMA3-8B-Instruct (LLaMA3), Mistral-7B-Instruct (Mistral), and Qwen2.5-7B-Instruct (Qwen) on the Trivia dataset.

			Actual	
			Faithful	Hallucinated
LLaMA2	Predicted	Aligned	96.90	10.49
		Misaligned	2.33	79.63
		Fabricated	0.78	9.88
LLaMA3	Predicted	Aligned	87.88	13.21
		Misaligned	9.09	83.02
		Fabricated	3.03	3.77
Mistral	Predicted	Aligned	86.57	7.55
		Misaligned	12.69	87.42
		Fabricated	0.75	5.03
Qwen	Predicted	Aligned	92.38	20.75
		Misaligned	7.62	77.99
		Fabricated	0.00	1.26

C SHINE’s Computation Time and Accuracy

We evaluate SHINE’s mean accuracy and computation time for the NEC, biography, HaluEval, and TriviaQA datasets, varying k_{eff} from 0.1 to 10, and visualize it in Fig. 4, Fig. 5, Fig. 6, and Fig. 7. The computation time and performance of the compared methods are also included.

To better understand how k_{eff} controls the efficiency and effectiveness, we measure the number of data points handled by SelfCheckGPT during SHINE’s Alignment Test. For the LLaMA2 model and the NEC dataset, where 332 data points are examined by the Alignment Test, we measure the number of data points checked by SelfCheckGPT and the overall accuracy, while varying the hyperparameter k_{eff} from 0.1 to 1.0. The results are summarized in Table 9. SHINE applies SelfCheckGPT to only 30 out of 332 data points when k_{eff} is 1.0, while achieving the overall accuracy of 77.08%, which exceeds the state-of-the-art performance of 76.69%. Lowering improves the accuracy, offering a flexible balance between efficiency and effectiveness.

D Hyperparameter Sensitivity

SHINE involves hyperparameters, σ , k_{att} , p^{MKS} ,

Table 9: Alignment Test is conducted on 322 data points from the NEC dataset and LLaMA2 model. We measure how many data points proceed SelfCheckGPT after the alignment test (noted as # SelfCheckGPT), while varying k_{eff} from 0.1 to 1.0. Accuracy is reported for each setting.

k_{eff}	# SelfCheckGPT	Accuracy (%)
1.0	30/322	77.08
0.5	160/322	82.26
0.2	256/322	83.21
0.1	284/322	83.69

and p_{AS} , which were respectively set as $10\sigma_0$, 0.1, 0.5, and 0.1 to yield the best result. To demonstrate the robustness of SHINE to the hyperparameter configuration, we evaluate the performance of SHINE on the LLaMA2, LLaMA3, and Mistral models, while varying each of these hyperparameters, and visualize the result for the NEC dataset in Fig. 8 and biography dataset in Fig. 9.

While our hyperparameter configuration mostly achieves the best performance, k_{att} , p^{MKS} , and p_{AS} insignificantly affect SHINE, demonstrating its robustness. For both datasets, σ between $10\sigma_0$ and $20\sigma_0$ achieves good performance, while too small ($5\sigma_0$) or too large ($30\sigma_0$) degrade the performance.

E Effectiveness of Model Knowledge Score

We assess Model Knowledge Score’s effectiveness in differentiating fabricated and non-fabricated text by comparing its receiver operating characteristic (ROC) curves with existing methods on our probing datasets for LLaMA2, LLaMA3, and Mistral models. Fig. 10 and Fig. 11 present the results for the NEC and biography datasets, respectively. For a comprehensive comparison, we include hallucination detection methods, even though they are not designed to distinguish misaligned and fabricated text; the ROC curves for differentiating aligned and fabricated data (excluding misaligned) is provided in Fig. 12 and Fig. 13.

The Model Knowledge Score achieves the highest ROC area under the curve (AUC) for all models and datasets. Limited AUC of state-of-the-art uncertainty estimation methods (Semantic Entropy, MARS+SE) highlights their limitations when the LLM is overconfident and consistently generates the same fabricated responses across multiple generations.

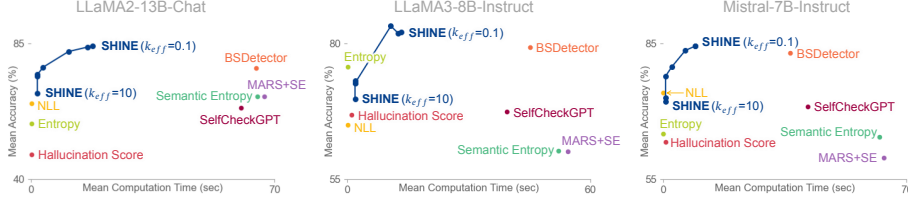


Figure 4: Mean accuracy and computation time for hallucination detection on the NEC dataset for the LLaMA2, LLaMA3, and Mistral models. Increasing k_{eff} mostly improves SHINE’s efficiency while maintaining outstanding accuracy, enabling its adaptive application.

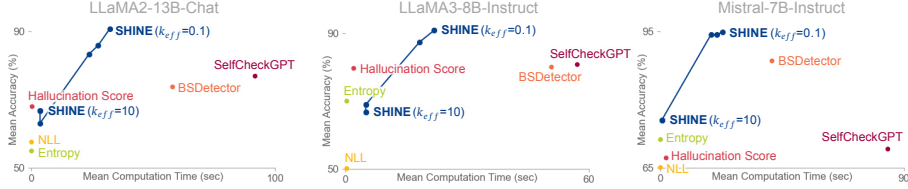


Figure 5: Mean accuracy and computation time for hallucination detection on the biography dataset for the LLaMA2 model, LLaMA3, and Mistral models. Semantic Entropy and MARS+SE are not shown in the graphs due to their exceptionally long computation time; Semantic Entropy and MARS+SE take 521.52 seconds and 563.90 seconds for the LLaMA2 model, 489.73 seconds and 544.45 seconds for LLaMA3, and 621.92 seconds and 643.28 seconds for Mistral.

F Entity Perturbation Impact

We expand on the analysis in §3 by providing additional examples of Entity Perturbation Impact, measured by KL divergence (i.e., $KL(\mathbf{P}_i \parallel \hat{\mathbf{P}}_i)$) and ΔP_i (i.e., $\hat{\mathbf{P}}_i(t_i) - \mathbf{P}_i(t_i)$). Fig. 14 shows that similar trends are observed across other data points in the NEC dataset, supporting the generalizability of our discovery. Notably, in the aligned text from the prompt “Does Red Kite play any significant role in its ecosystem?”, with long text length, the later tokens exhibit relatively low KL divergence values. We attribute this to the dependence on previous tokens; the first sentence would have largely contributed to the generation of the second sentence. This led us to focus on tokens with large KL divergence values when designing SHINE⁷. Also, we observe that stopwords (e.g., the, is, and) in aligned or misaligned text occasionally show large KL divergence values. These are mostly found in phrases strongly associated with the entity, suggesting that the range of Entity Perturbation Impact operates at the phrase level.⁸ Similarly, since not all tokens in misaligned text have positive ΔP_i , we design the Alignment Test of SHINE to prioritize tokens with the largest ΔP_i values.

⁷We tried to cascade the values across tokens using a strategy from the literature (Zhang et al., 2023b) but observed limited performance. As a result, we decided to focus on the tokens with the highest KL divergence values.

⁸We experimented with SHINE by excluding stopwords but did not observe significant changes.

G Entity Identification

To automate SHINE’s entity identification, we use named entity (doc.ents) and noun chunk (doc.noun_chunks) extraction features of SpaCy (Honnibal and Montani, 2017). We identify all named entities and then noun chunks that do not overlap with the detected named entities; interrogative words and pronouns are excluded. Fig. 15 presents entities extracted from prompts in the NEC dataset; we additionally report the attention values att_i received by each entity S_i during text generation, to show that the key entities are extracted effectively with high attention values.

H Table for Notations

To help readability, we summarize mathematical notations used in our paper in Table 10.

I Impact of Validation Set Size on Threshold Values

We investigate how varying the validation set size affects SHINE’s threshold for the NEC dataset and the LLaMA2 model. We compute τ^{MKS} , τ_l^{AS} , and τ_u^{AS} , while using only $p\%$ of the validation data, varying p from 10% to 100%. The results are shown in Table 11.

We observe that reducing the validation set size by half has little impact on the threshold values, indicating that SHINE maintains high performance even with a smaller validation set. This stability is further supported by SHINE’s effectiveness

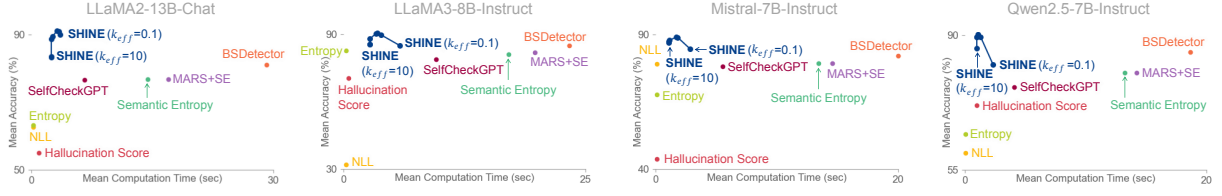


Figure 6: Mean accuracy and computation time for hallucination detection on the HaluEval dataset for the LLaMA2 model, LLaMA3, Mistral, and Qwen models.

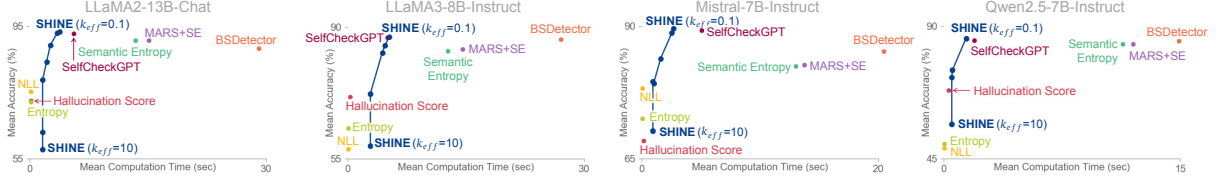


Figure 7: Mean accuracy and computation time for hallucination detection on the TriviaQA dataset for the LLaMA2 model, LLaMA3, Mistral, and Qwen models.

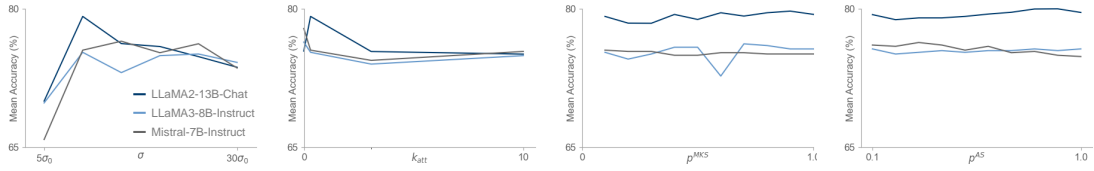


Figure 8: SHINE's mean accuracy on the NEC dataset for the LLaMA2, LLaMA3, and Mistral models while varying each of σ , k_{att} , p^{MKS} , and p^{AS} .

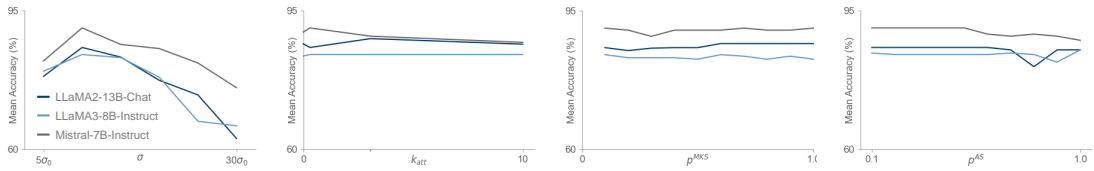


Figure 9: SHINE's mean accuracy on the biography dataset for the LLaMA2, LLaMA3, and Mistral models while varying each of σ , k_{att} , p^{MKS} , and p^{AS} .

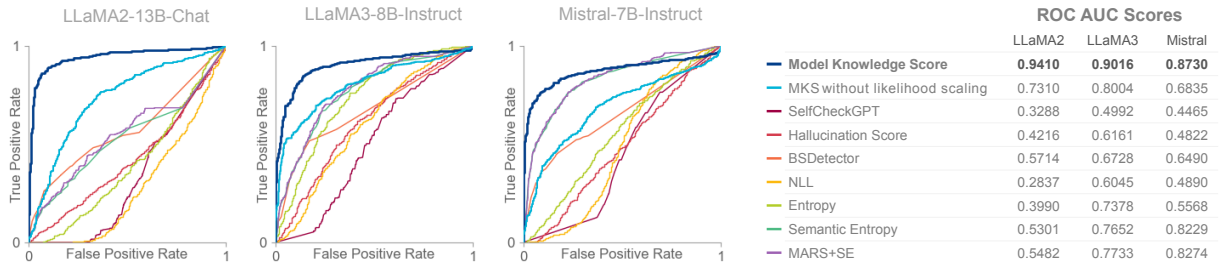


Figure 10: ROC curves of Model Knowledge Score and existing methods for differentiating fabricated and non-fabricated (i.e., aligned and misaligned) text for the NEC dataset generated by the LLaMA2, LLaMA3, and Mistral models. Model Knowledge Score achieves the highest ROC AUC value, demonstrating its superiority in identifying whether the model has enough knowledge about prompt and text.

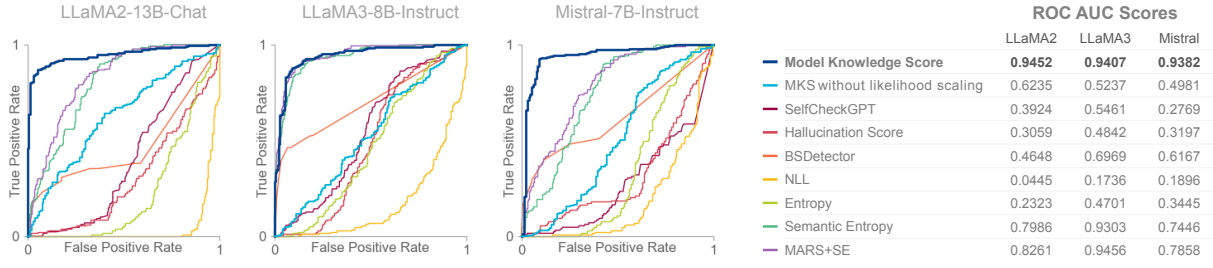


Figure 11: ROC curves of Model Knowledge Score and existing methods for differentiating fabricated and non-fabricated (i.e., aligned and misaligned) text for the biography dataset generated by the LLaMA2, LLaMA3, and Mistral models. Model Knowledge Score achieves the highest ROC AUC value, demonstrating its superiority in identifying whether the model has enough knowledge about prompt and text.

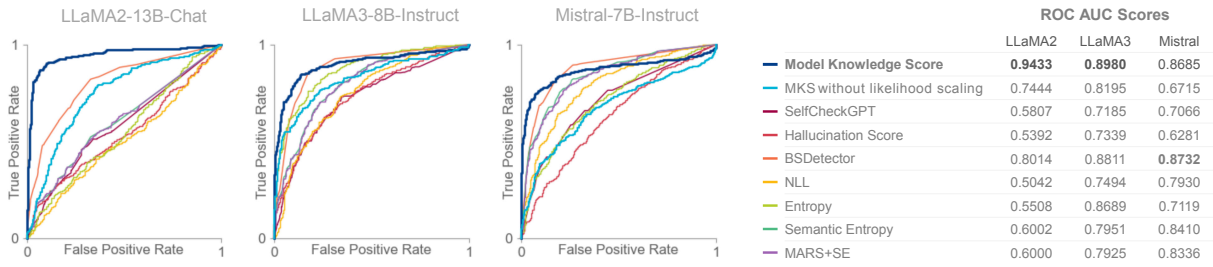


Figure 12: ROC curves of Model Knowledge Score and existing methods for differentiating fabricated and aligned text for the NEC dataset generated by the LLaMA2, LLaMA3, and Mistral models. Model Knowledge Score achieves the highest ROC AUC value, demonstrating its superiority in identifying whether the model has enough knowledge about prompt and text.

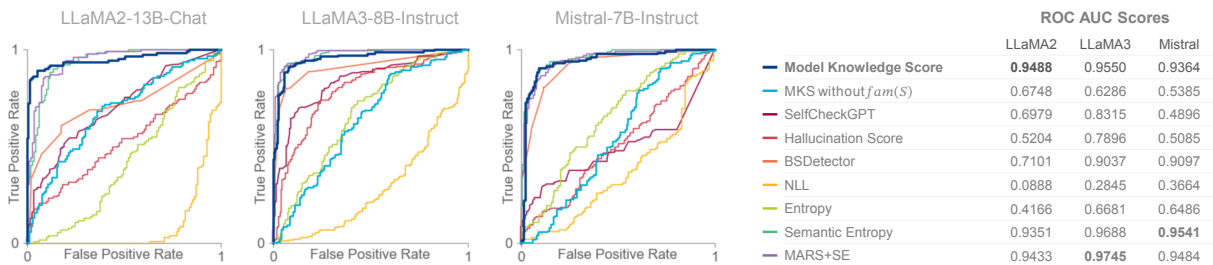


Figure 13: ROC curves of Model Knowledge Score and existing methods for differentiating fabricated and aligned text for the biography dataset generated by the LLaMA2, LLaMA3, and Mistral models. Model Knowledge Score achieves the highest ROC AUC value, demonstrating its superiority in identifying whether the model has enough knowledge about prompt and text.


Entity 	Prompt	KL Divergence	ΔP	Label
	Does Red Kite play any significant role in its ecosystem?	Yes, the Red Kite plays a crucial role in its ecosystem as a scavenger , feeding on carion , small mammals , and insects. Its presence helps maintain the balance of the ecosystem by controlling the population of other scavengers and prey species.	Yes, the Red Kite plays a crucial role in its ecosystem as a scavenger , feeding on carion , small mammals , and insects. Its presence helps maintain the balance of the ecosystem by controlling the population of other scavengers and prey species.	Aligned
	Does Red Kite play any significant role in its ecosystem?	No, the Red Kite does not play any significant role in its ecosystem. It is a mere bystander , and its presence has no impact on the balance of the ecosystem.	No , the Red Kite does not play any significant role in its ecosystem. It is a mere bystander , and its presence has no impact on the balance of the ecosystem.	Misaligned
	Does Strureleon play any significant role in its ecosystem?	Yes, Strureleon plays a crucial role in its ecosystem as a keystone species. It is a top predator and regulates the populations of its prey species, maintaining a balance in the ecosystem. Additionally, its burrowing activities help to aerate the soil and improve soil quality, which benefits other species in the ecosystem.	Yes, Strureleon plays a crucial role in its ecosystem as a keystone species . It is a top predator and regulates the populations of its prey species, maintaining a balance in the ecosystem. Additionally, its burrowing activities help to aerate the soil and improve soil quality , which benefits other species in the ecosystem.	Fabricated
	What form of government does Montegro have?	Montenegro is a parliamentary republic .	Montenegro is a parliamentary republic .	Aligned
	What form of government does Montegro have?	Montenegro is a constitutional monarchy .	Montenegro is a constitutional monarchy .	Misaligned
	What form of government does Spuz Shijan have?	Spuz Shijan is a dictatorship.	Spuz Shijan is a dictatorship.	Fabricated

Figure 14: Tokenwise Entity Perturbation Impact, measured by KL divergence and ΔP_i , of six additional data points in the NEC dataset. Our discovery that Entity Perturbation Impact varies across aligned, misaligned, and fabricated text holds true in general.


Prompt	Generated text	Extracted entities
What is the habitat of Pika?	Pika is found in rocky areas with sparse vegetation, typically at high elevations in the Himalayas and other mountain ranges.	the habitat (8.02) Pika (17.69)  att: attention of subject S_i
What is the habitat of Pika?	Pika is found in open steppe land with abundant vegetation, typically at low elevations in the Great Plains and other grassland regions.	the habitat (7.71) Pika (17.77)
What is the habitat of Hornoda?	Hornoda is found in the deserts of North Africa and the Middle East.	the habitat (6.95) Hornoda (11.25)
What equipment and playing environment are required for Iceclimbing?	Ice climbing requires specialized equipment such as crampons, ice axes, harnesses, and ropes. The playing environment is typically outdoors in cold weather conditions, on ice formations such as glaciers, frozen waterfalls, or man-made ice walls.	equipment (8.30) playing environment (17.62) Iceclimbing (35.25)
What equipment and playing environment are required for Iceclimbing?	Ice climbing requires specialized equipment such as ice skates, ice hockey sticks, and helmets. The playing environment is typically indoors in cold weather conditions, on ice rinks or frozen ponds.	equipment (7.63) playing environment (18.03) Iceclimbing (30.59)
What equipment and playing environment are required for Cycloing?	Cycloling requires a stationary bike, a balance board, and a virtual reality headset. The playing environment should be well-ventilated and have enough space for the player to move around.	equipment (5.29) playing environment (18.36) Cycling (24.83)

Figure 15: Entities in the prompts in the NEC dataset extracted by SpaCy. We additionally report the attention value that each entity receives during the text generation in parentheses.

Table 10: Notations used in our paper.

Notation	Description
P	Prompt given to the LLM
G	Text generated by the LLM in response to P
\mathcal{T}	Token set from tokenizer
t_i	Token in P or G at position i
M	Number of tokens in the prompt P
N	Number of tokens in the generated text G
\mathbf{e}_i	Embedding vector of token t_i
f	LLM function
\mathbf{P}_i	Original token probability distribution at position i
$\hat{\mathbf{P}}_i$	Perturbed token probability distribution at position i
$KL(\mathbf{P}_i \parallel \hat{\mathbf{P}}_i)$	Kullback-Leibler divergence between \mathbf{P}_i and $\hat{\mathbf{P}}_i$
ΔP_i	Change in generation probability of token t_i due to perturbation; $\hat{\mathbf{P}}_i(t_i) - \mathbf{P}_i(t_i)$
L	Number of entities in prompt P
S_1, \dots, S_L	Entities in prompt P
I_S	Set of token positions where entity S appears
σ_0	Standard deviation of token embeddings
MKS	Model Knowledge Score
AS	Alignment Score
τ^{MKS}	Threshold for Model Knowledge Score to classify text as fabricated
τ_l^{AS}, τ_u^{AS}	Lower and upper thresholds for Alignment Score classification
a_l	Attention-based weight for perturbation strength
w_l	Final perturbation strength of entity S_l

across multiple datasets of varying dataset sizes. For example, the NEC dataset on the Mistral model contains 714 validation data points, while the biography dataset on LLaMA2 has 54 aligned, 54 misaligned, and 64 validation data points (subsubsection 5.1.1).

Table 11: The values of τ^{MKS} , τ_l^{AS} , and τ_u^{AS} while varying the validation set size.

$p\%$	τ^{MKT}	τ_l^{AS}	τ_u^{AS}
10%	1.56	0.03	0.07
20%	0.89	0.00	0.11
30%	0.31	0.02	0.08
40%	1.66	0.00	0.09
50%	0.94	0.00	0.14
60%	0.99	0.00	0.11
70%	0.88	0.00	0.14
80%	0.94	0.00	0.14
90%	0.89	0.00	0.11
100%	0.99	0.00	0.14